

A Fluorescent Sensor For Zn²⁺ Based on Rhodamine Thiophene Framework

Cui-Bing Bai^{1,2}, Sheng-Nan Wang¹, Rui Qiao^{1,2,*}, Hai-Yun Fan¹, Biao Wei^{1,2}, Peng Xu¹, Lin Zhang^{1,2}, Jie Zhang¹, Rui-Qian Li^{1,2}, Shui-Sheng Chen^{1,2}, Song Yang^{1,2}

¹ School of Chemistry and Materials Engineering, Fuyang Normal University, Fuyang, Anhui Province, 236037, China

² Anhui Province Key Laboratory for Degradation and Monitoring of Pollution of the Environment, 236037, China

*E-mail: qiaorui@mail.ipc.ac.cn

Received: 15 June 2018 / Accepted: 18 August 2018 / Published: 1 October 2018

The thiophene-modified rhodamine derivative was synthesized and characterized. The fluorescent sensor **XQS** for Zn²⁺ have been studied. **XQS** showed fluorescent specific selectivity for Zn²⁺ against other metal ions in HEPES buffer (10 mM, pH 7.4)/CH₃CN (40:60, V/V) solution. The distinct color change and the rapid emergence of fluorescence emission provided naked-eyes detection for Zn²⁺. The test strip results showed that the sensor **XQS** could act as a convenient Zn²⁺ test kit. The recognition mechanism of **XQS** toward Zn²⁺ was studied by IR, the Job's plots and ESI-MS analysis. The detection limits of **XQS** towards Zn²⁺ was calculated as 6.89 μM. **XQS**-Zn²⁺. In addition, cyclic voltammograms of **XQS** and **XQS**+Zn²⁺, fluorescence lifetime and fluorescence quantum yield were also determined.

Keywords: Rhodamine-6G; Fluorescent Sensors; Zn²⁺; Test Strip.

1. INTRODUCTION

The exploration of fluorescent sensors for the detection of metal ions have been received extensively attention in the last few decades [1-6]. Amongst the important transition metal ions, Zn²⁺ is known for their ability in comprehensive applications [7-10]. Meanwhile, the disruption of Zn²⁺ is dangerous to human health. For example, the disbalance of Zn²⁺ has been entwined with hypoxia ischemia, epilepsy and several neurological disorders [11-13]. So, it is absolutely necessary to develop the effective method to detect Zn²⁺ [14-16].

Fluorescent sensors which are capable of selectively recognizing guest species are of particular interest in supramolecular chemistry to check trace amount of transition metal ions in the last decades

[17, 18]. Because of low cost and high sensitivity, the research efforts have been paid attention to the design and synthesize novel sensors.

In recent years, the rhodamine-6G platform is widely used as fluorescent sensors by many investigators [19]. In particular, the modified spirolactam structure which enables colorless and nonfluorescent can be changed into the colored and highly fluorescent ring-opened amide form in the presence of the corresponding metal ions [20]. In order to improve the sensitivity and selectivity of fluorescent chemosensor, some heterocycles have been used to modify the rhodamine platform including thiophene, pyrrole and furan [21, 22]. However, most of them are designed through C=N by aromatic aldehydes reacting with rhodamine-6G amine derivatives [23-25]. But few fluorescent sensors linked by amide between heterocycles and rhodamine-6G have been reported. It is clear that the rhodamine-6G derivatives modified by amide have more potential coordination sites to bind metal ions than by C=N, which may enhance sensitivity and selectivity.

In this paper, the novel fluorescent chemosensor **XQS** was designed and synthesized (Scheme 1), which was modified by thiophene structure in use of amide. To our surprised, the fluorescent sensor **XQS** could “naked-eye” recognize Zn^{2+} in HEPES buffer (10 mM, pH 7.4)/CH₃CN (40:60, V/V). Meanwhile, other cations such as Fe^{3+} , Cr^{3+} , Hg^{2+} , Ag^+ , Ca^{2+} , Cu^{2+} , Pb^{2+} , Cd^{2+} , Ni^{2+} , Co^{2+} and Mg^{2+} could not cause any interference. In addition, cyclic voltammograms of **XQS** and **XQS**+ Zn^{2+} , fluorescence lifetime and fluorescence quantum yield were also determined.

2. EXPERIMENTAL

2.1. General methods of UV-Vis spectroscopy and fluorescent spectroscopy

The UV-vis spectra were measured on the Shimadzu UV-1601 spectrometer. And the fluorescent spectra were recorded by the HORIBA FLUOROMAX-4-NIR spectrometer. The **XQS** concentration was held invariably (3.3×10^{-4} M). The metal ions solution were prepared from the corresponding metal nitrate.

¹H NMR and ¹³C NMR spectra were tested on the Bruker at 400 MHz using TMS as an internal standard, DMSO-*d*₆ as the solvents. Melting points were examined on an X-4 digital melting-point apparatus (uncorrected). Infrared spectra were obtained on a Nicolet 5700 FT-IR spectrophotometer. Solvents were purified and dried using standard protocol; the other chemical reagents were obtained commercially and used as received without further purification. All reagents were used of analytical grade.

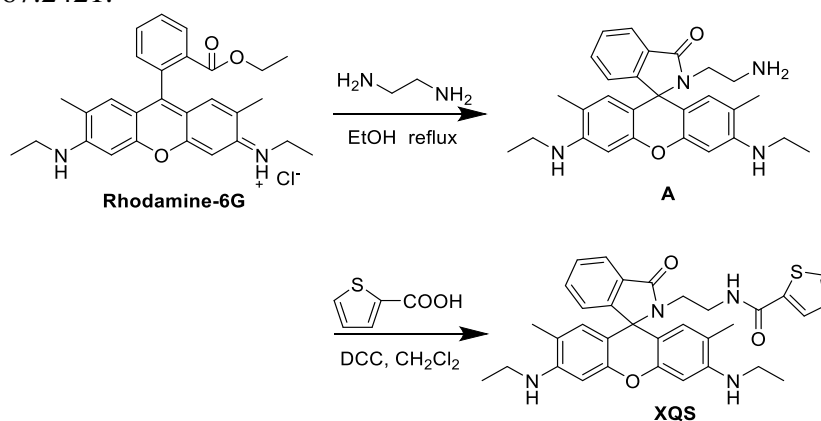
2.2. Cyclic voltammetry

Cyclic voltammetry (CV) was performed on CHI660E potentiostat in a three-electrode electrochemical cell with a 1 mm sized home-made glassy carbon electrode (Goodfellow) used as a working electrode, saturated calomel electrode (SCE, Radiometer) as a reference electrode, and a platinum wire (Goodfellow) as a counter electrode. The reference electrode was separated from the

bulk solution by a fritted-glass bridge filled with the solution of supporting electrolyte (0.1 M TBA·BF₄ in CH₃CN). CV experiments were measured at room temperature.

2.3. Synthesis of chemosensor XQS

Chemosensor **XQS** was synthesized as Scheme 1. According to the previous procedure, compound **A** was received.¹⁷ 2-Thiophenecarboxylic acid (10 mmol), DCC (dicyclohexylcarbodiimide) (20 mmol) and compound **A** (10 mmol) were dissolved in dichloromethane (10 mL) in a 25 mL round flask. The mixture was reacted for 12h at the ambient temperature. When the solvent was evaporated under reduced pressure, the crude product was purified by silica gel chromatography (ethyl acetate: petroleum ether = 1: 2) to get chemosensor **XQS**. Yield 81%, m.p. >300 °C, ¹H NMR (DMSO-*d*₆, 400 MHz) δ 8.33 (t, *J*=5.4 Hz, 1H), 7.81 (dd, *J*=5.8, 2.8 Hz, 1H), 7.69 (dd, *J*=4.9, 0.8 Hz, 1H), 7.61-7.55 (m, 1H), 7.53-7.45 (m, 2H), 7.08 (dd, *J*=4.9, 3.8 Hz, 1H), 6.95 (dd, *J*=5.8, 2.6 Hz, 1H), 6.27 (s, 2H), 6.13 (s, 2H), 5.06 (t, *J*=5.3 Hz, 2H), 3.24-3.07 (m, 7H), 2.99 (dd, *J*=8.5, 5.4 Hz, 2H), 1.85 (s, 6H), 1.21 (t, *J*=7.1 Hz, 6H). ¹³C NMR (100 MHz, DMSO) δ 167.96, 161.28, 157.08, 154.41, 151.40, 148.11, 140.18, 133.22, 131.06, 130.44, 128.66, 128.30, 128.23, 127.86, 124.11, 124.05, 122.88, 122.81, 118.76, 104.80, 96.16, 64.86, 37.95, 17.47, 14.64. HRMS (ESI) *m/z*: [M+H]⁺ Calcd for C₃₃H₃₄N₄O₃S: 567.2424; Found 567.2421.



Scheme 1. Synthetic route to fluorescent sensor **XQS**.

3. RESULTS AND DISCUSSION

3.1. Spectral studies of chemosensor XQS

The spectral responses of compound **XQS** to various metal cations including Ag⁺, Fe³⁺, Cr³⁺, Hg²⁺, Ca²⁺, Zn²⁺, Cu²⁺, Pb²⁺, Cd²⁺, Ni²⁺, Co²⁺ and Mg²⁺ were investigated in HEPES buffer (10 mM, pH 7.4)/CH₃CN (40:60, V/V) by UV-vis and fluorescence spectroscopy. To chemosensor **XQS**, any absorption was not detected above 500 nm. When Zn²⁺ was added into the solution of **XQS**, the colorless solution changed to yellow-green at once (Fig. 1). Meanwhile, a new absorption peak at 525 nm appeared. But the other metal ions could not cause the **XQS** solution color change except Fe³⁺ and Hg²⁺. Although Fe³⁺ and Hg²⁺ also led to color changes, their changes are less pronounced effect than

Zn²⁺. It indicated that only Zn²⁺ could cause the spirolactam of rhodamine to be open. And the results exhibited that **XQS** could discriminate Zn²⁺ from other ions.

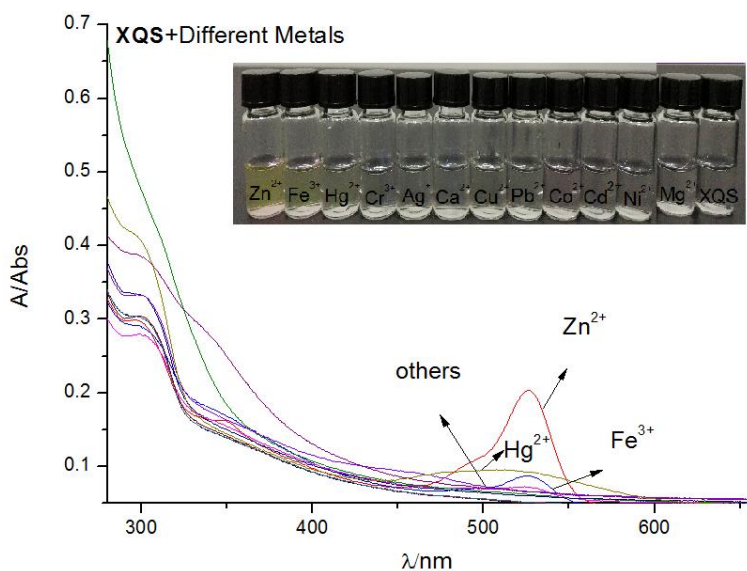


Figure 1. Absorption spectra of the sensor **XQS** (3.3×10^{-4} M) in the presence of various metal ions in HEPES buffer (10 mM, pH 7.4)/CH₃CN (40:60, V/V). Inset: Photographs of chemosensor **XQS** (3.3×10^{-4} M) in the presence of various metal ions in HEPES buffer (10 mM, pH 7.4)/CH₃CN (40:60, V/V).

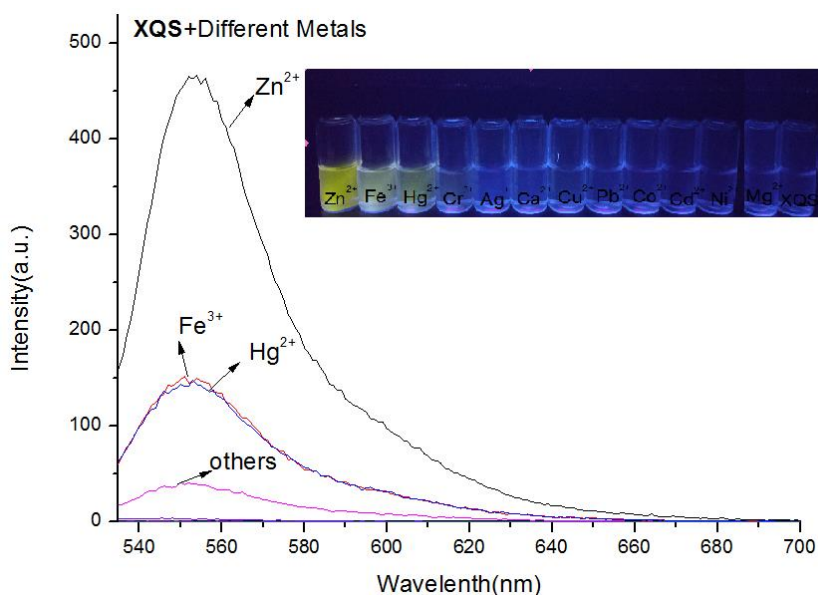


Figure 2. Fluorescence spectra changes of the sensor **XQS** (3.3×10^{-4} M) in the presence of various metal ions in HEPES buffer (10 mM, pH 7.4)/CH₃CN (40:60, V/V), $\lambda_{ex} = 525$ nm, detection from 540 to 720 nm. Inset: Photographs of chemosensor **XQS** (3.3×10^{-4} M) in the presence of various metal ions in HEPES buffer (10 mM, pH 7.4)/CH₃CN (40:60, V/V).

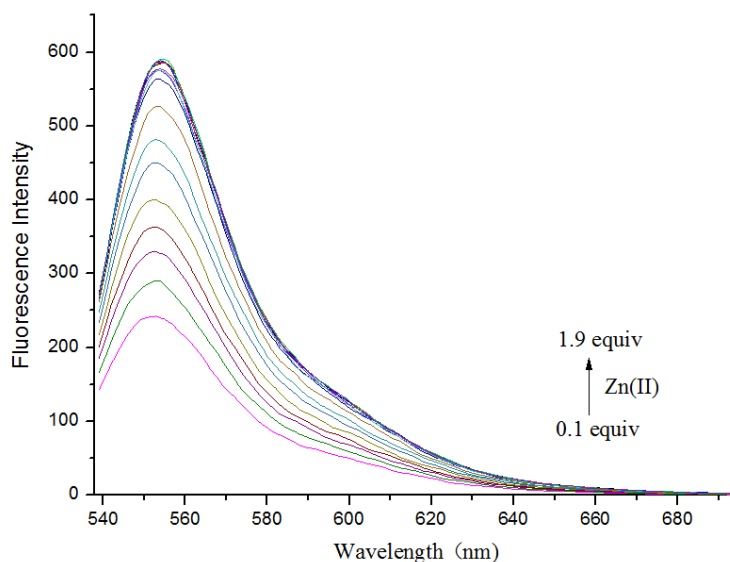


Figure 3. Fluorescence spectra of **XQS** (3.3×10^{-4} M) in the presence of different concentration of Zn^{2+} (0-1.9 equiv.) in HEPES buffer (10 mM, pH 7.4)/ CH_3CN (40:60, V/V), $\lambda_{\text{ex}} = 525$ nm, detection from 540 to 700 nm.

The fluorescent responses of **XQS** to various cations were also studied. When **XQS** was excited by 525 nm, any obvious fluorescent emission peak did not appear. Interestingly, the clear emission peak arose out at 550 nm by adding Zn^{2+} (Fig. 2). And it was found that the intensity at 550 nm was improved along with the concentration of Zn^{2+} (Fig. 3). Although only Fe^{3+} and Hg^{2+} among other ions were observed the same phenomenon, their fluorescence intensity at 550 nm was much lower (Fig. 2). From the above data, chemosensor **XQS** could discriminate Zn^{2+} from other cations by fluorescent spectrum. And it was conceived that the weak fluorescent intensity structure of spiro lactam was transformed into the strong fluorescent intensity ring-open amide form when Zn^{2+} was added.

In order to investigate the selectivity of **XQS** to Zn^{2+} , anti-interference experiments were applied. From Fig. 2 and Fig. 4, it was clear that the intensity at 550 nm caused by other cations was too weak to compare with that caused by Zn^{2+} . And it was found that the intensity change caused by chemosensor **XQS** was hardly affected by coexistent metal ions. So chemosensor **XQS** could interact with Zn^{2+} selectively. Moreover, the intensity at 550 nm was increased by degree when 20 equivalents of Zn^{2+} was added to the solution of chemosensor **XQS** (3.3×10^{-4} M). After 30 min, the intensity was steady. So the interaction between **XQS** and Zn^{2+} completed within 30 min when 20 equivalents of Zn^{2+} was added to the solution of chemosensor **XQS** (3.3×10^{-4} M) (see SI Fig. S4).

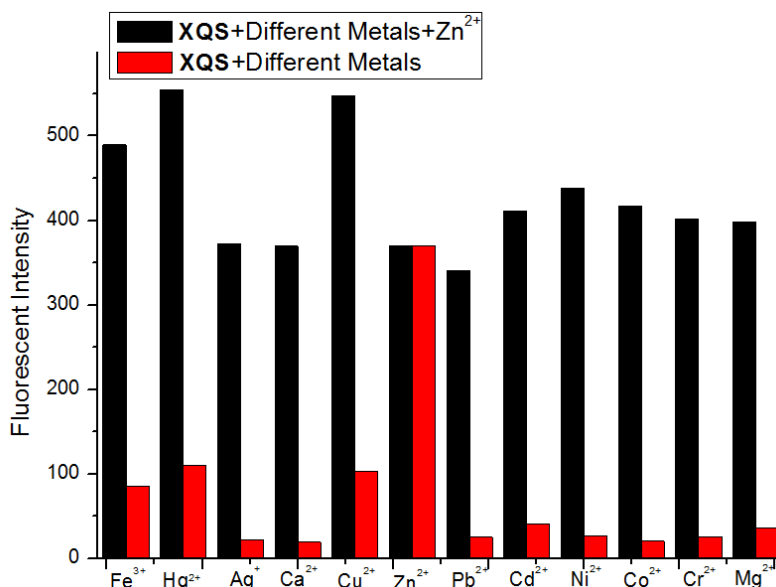


Figure 4. Fluorescence response of **XQS** (3.3×10^{-4} M) in HEPES buffer (10 mM, pH 7.4)/CH₃CN (40:60, V/V) at 550 nm upon addition of respective metal ions, followed by addition of Zn²⁺ (1.5 equiv.), $\lambda_{\text{ex}} = 525$ nm. The anti-interference of **XQS** (3.3×10^{-4} M) for Zn²⁺ (1.5 equiv.) detection was carried out by adding a mixture of other metal ions and Zn²⁺ to the sensor solution.

To verify the stoichiometry between **XQS** and Zn²⁺, fluorescence titrimetric method and Job's plots analyses and IR analyses were performed. According to the data, the stoichiometric ratio between them was 1:1 (see SI Fig. S5 and Fig. S6).

Based on the IR spectra, the mechanism of the interaction between **XQS** and Zn²⁺ was discussed. When **XQS** interacted with Zn²⁺, the stretching vibration absorption peak which belonged to N-H at 3432cm^{-1} disappeared. And new absorption peaks emerged at 1608cm^{-1} and 1650cm^{-1} , which belonged to the stretching vibration of C=N. Because the spiro lactam ring of **XQS** was open once **XQS** interacted with Zn²⁺. And the amido bond (O=C-N-H) was deprotonated and tautomerized to carbon-nitrogen double bond (C=N). In addition, the peak at 1384cm^{-1} belonged to NO₃⁻. So, chemosensor **XQS** might chelate with Zn²⁺ *via* N, O-donor atoms as shown in Scheme 2. The interaction between them was further approved by ESI-MS. From mass spectra, the ion peaks at m/z 675.6763 was identical to [**XQS**+Zn²⁺+NO₃⁻-H₂O+H⁺]⁺ (see SI Fig. S3).

From Scheme 2, it showed that the ring-closed spiro lactam transformed to the ring-opened amide form once Zn²⁺ was added into the solution of **XQS**. So the colorless solution of **XQS** changed to yellow-green. And the new absorption peak at 525 nm appeared. Meanwhile, the emission peak at 550 nm arose when the solution of **XQS** was excited at 525 nm. Besides, the detection limit of chemosensor **XQS** towards Zn²⁺ was figured out as $6.89\ \mu\text{M}$ (see SI Table S1) [26]. And the binding constant was also calculated. Moreover, the fluorescent life time and the fluorescence quantum yield of **XQS**-Zn²⁺ were measured (see SI Table S1).

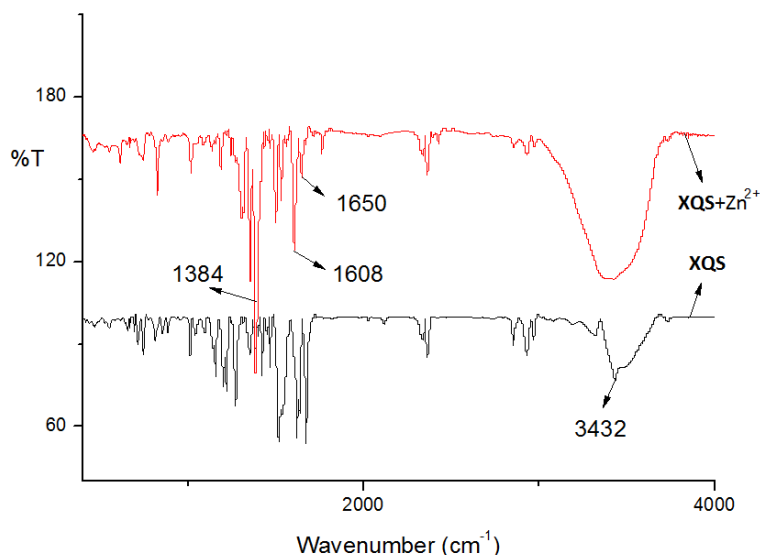
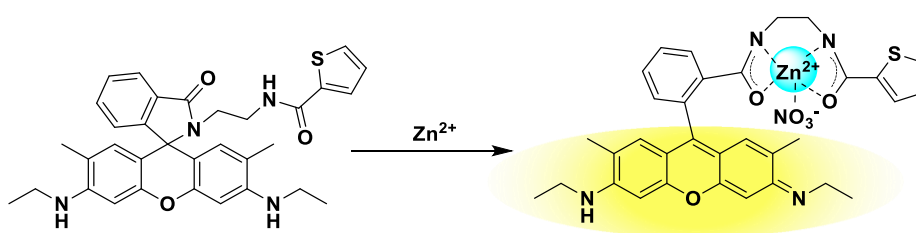


Figure 5. IR spectra of compound **XQS** and **XQS+Zn²⁺** complex in KBr disks.



Scheme 2. The proposed reaction between **XQS** and **Zn²⁺**.

In order to explore the application of **XQS** in practise, test strips were prepared after filter papers were immersed into a HEPES buffer (10 mM, pH 7.4)/CH₃CN (40:60, V/V) solutions of sensor **XQS** (6.6×10^{-4} M) and dried in the air. Then the obtained test strips were used to detect **Zn²⁺** (6.6×10^{-4} M). As shown in Fig. 6, the obvious color change was observed while the strips were irradiated by the 365 nm UV lamp. So, it indicated that chemosensor **XQS** could still recognize **Zn²⁺** by naked-eye in solid state as well.

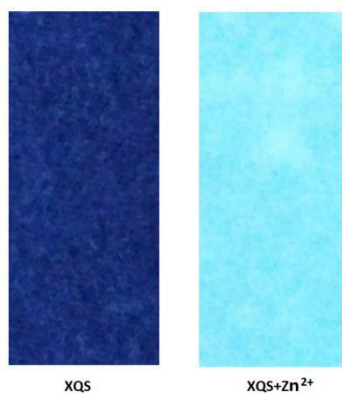


Figure 6. Photographs of **XQS** (6.6×10^{-4} M) on test papers under irradiation at 365 nm.

3.2. Electrochemistry

Cyclic voltammetry was used to investigate the electrochemical behavior of sensor **XQS** and **XQS**+ Zn^{2+} . As showed in figure 7, sensor **XQS** alone exhibited E_{1R} and E_{1O} at -0.94 V and -0.80 V, respectively. However, E_{2R} and E_{2O} for **XQS**+ Zn^{2+} were shifted to -1.06 V and -0.70 V when Zn^{2+} was added into the **XQS** solution. These notable shifts were displayed bonding attraction between the sensor **XQS** and Zn^{2+} [27, 28]. The results showed that sensor **XQS** explored some remarkable changes with Zn^{2+} , and also provided useful information about electrochemical sensing nature of sensor **XQS**.

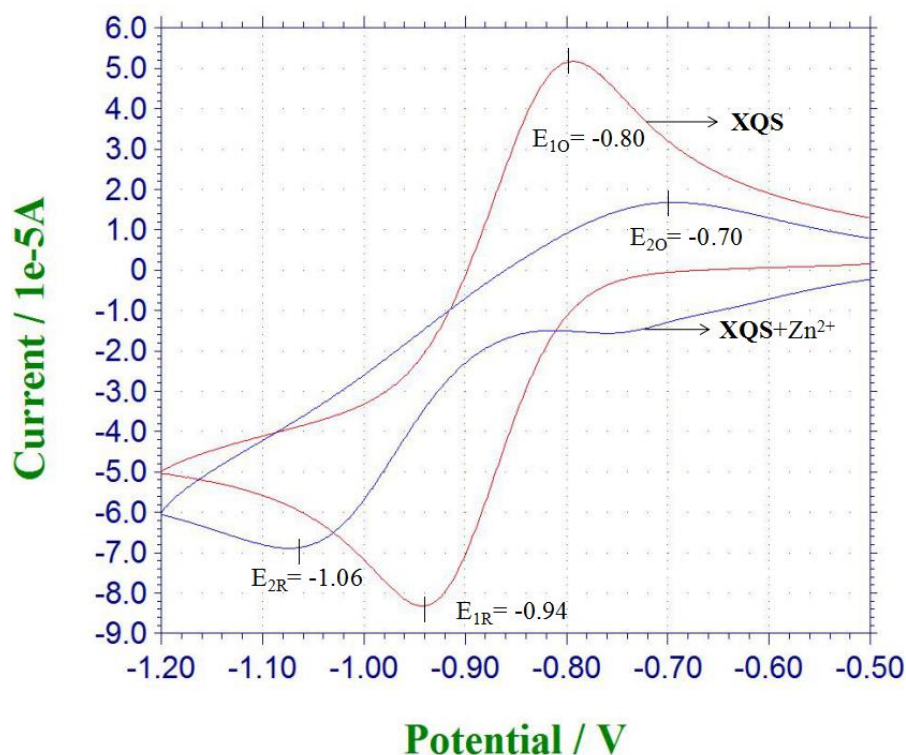


Figure 7. Cyclic voltammograms of **XQS** (0.2 mM) and **XQS**+ Zn^{2+} (0.2 mM) in $\text{CH}_3\text{CN}/ [\text{TBA}] [\text{BF}_4]$ (0.1 M), performed at a scan rate of 100 mV/s.

4. CONCLUSIONS

In summary, thiophene-modified chemosensor **XQS** based on rhodamine was synthesized and characterized. Chemosensor **XQS** could discriminate Zn^{2+} from other metal ions in HEPES buffer (10 mM, pH 7.4)/ CH_3CN (40:60, V/V) solution. The interaction between **XQS** and Zn^{2+} was studied based on different methods. Moreover, chemosensor **XQS** could still recognize Zn^{2+} effectively in solid state as well. All data indicated that thiophene-modified chemosensor **XQS** could identify potentially Zn^{2+} from other metal ions in physiological and environmental systems.

SUPPLEMENTARY MATERIAL

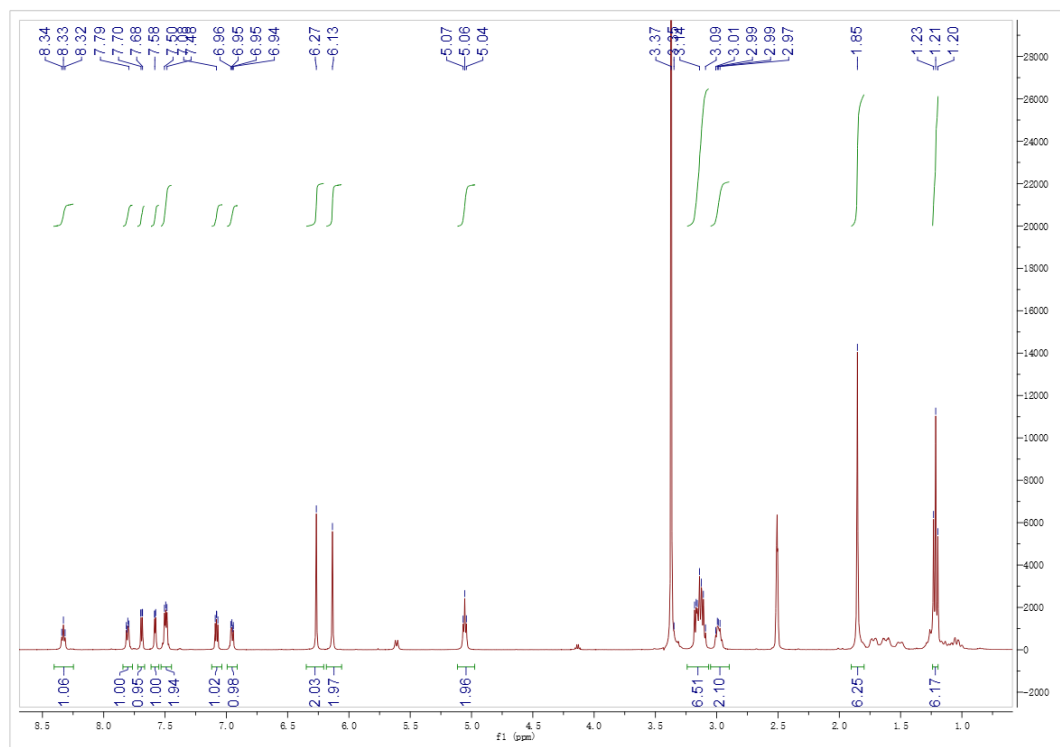


Fig. S1 ^1H NMR spectra of compound XQS.

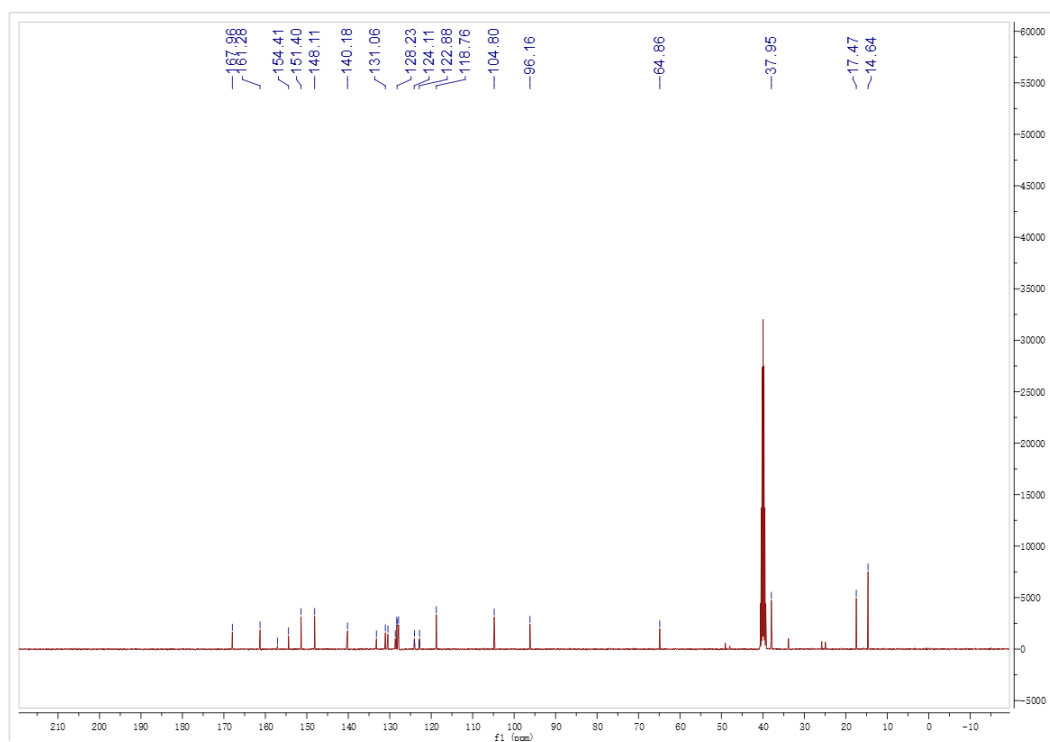


Fig. S2 ^{13}C NMR spectra of compound XQS.

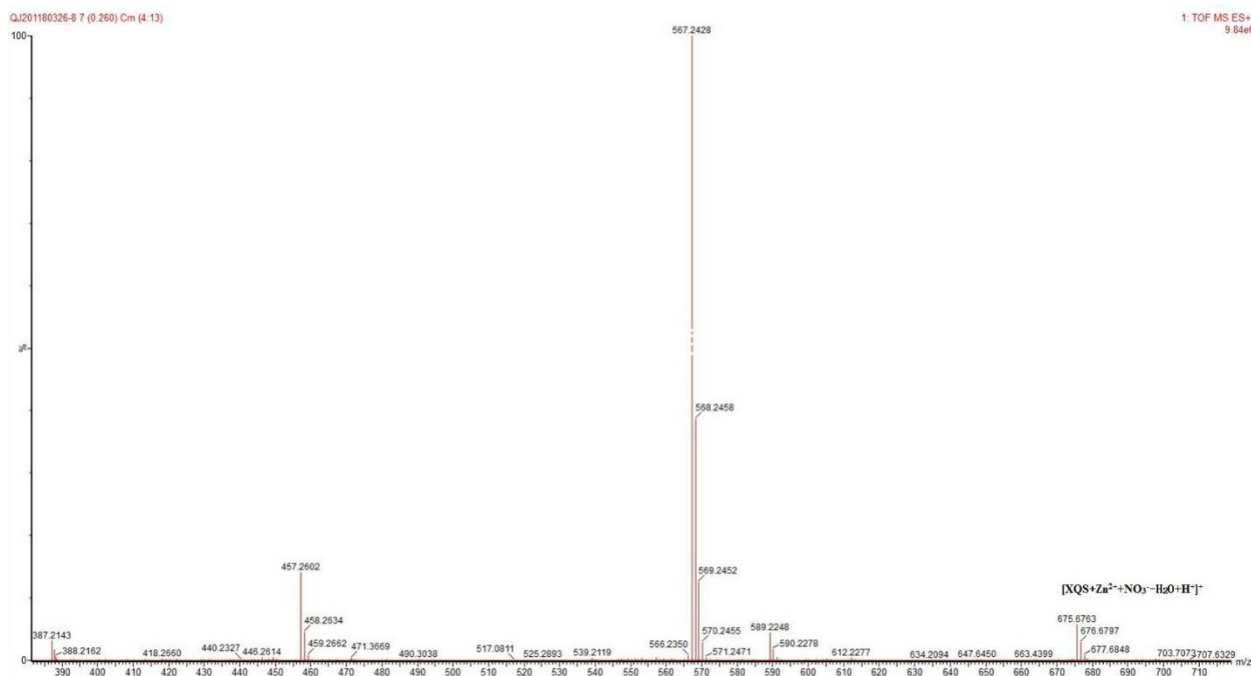
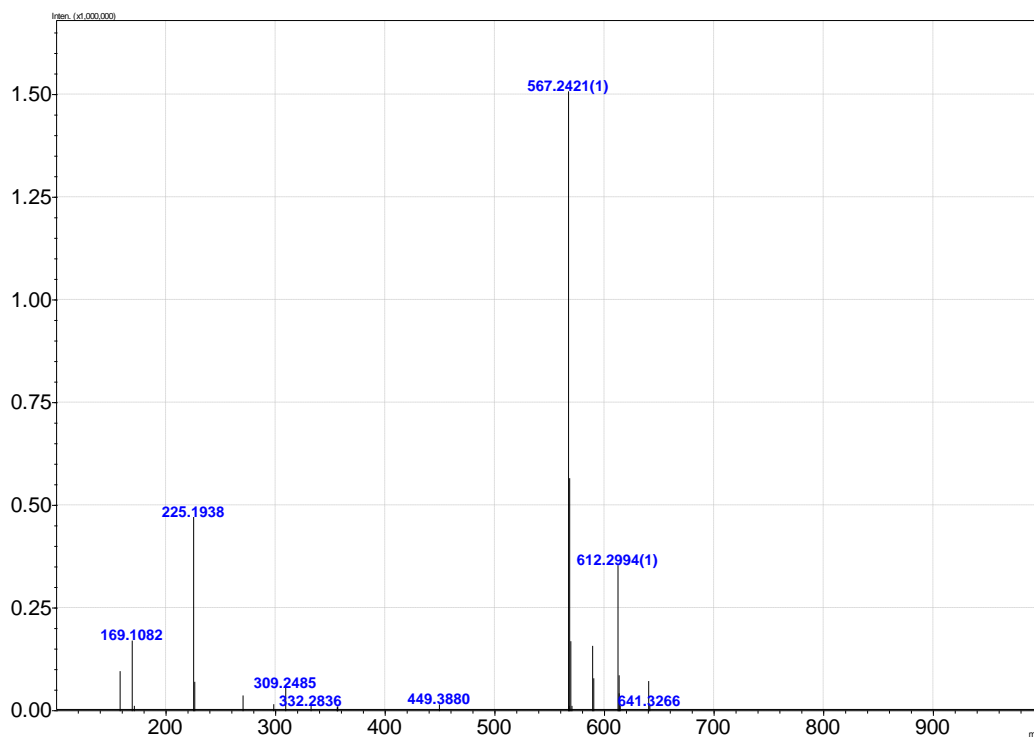


Fig. S3 ESI-MS spectrum of XQS and XQS-Zn²⁺.

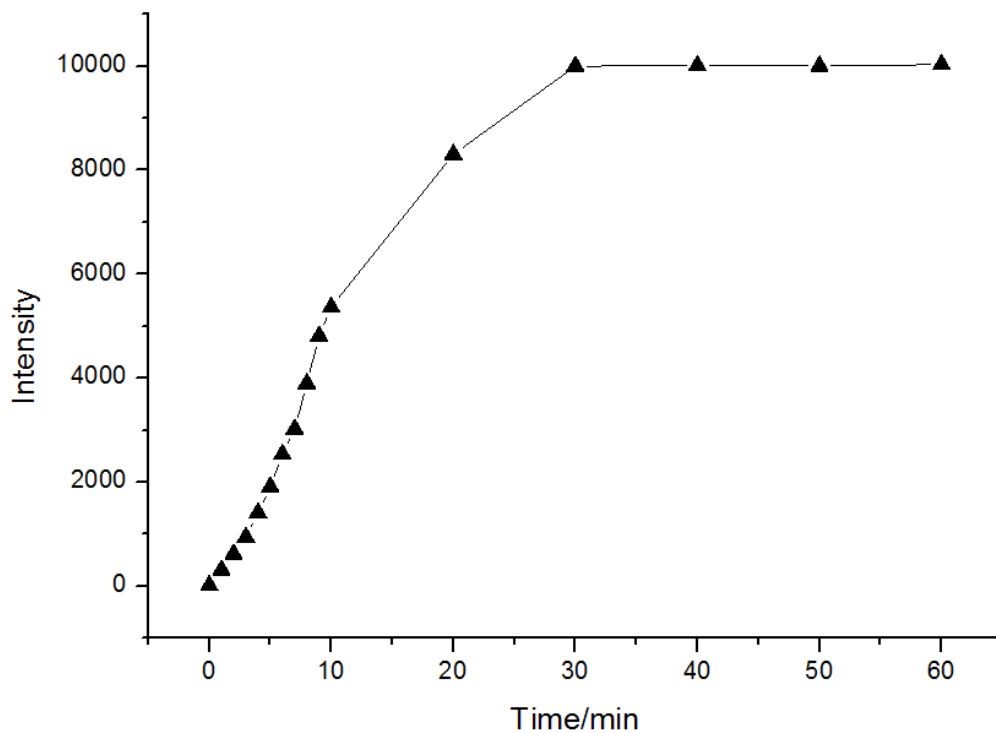


Fig. S4 Time-dependent changes of fluorescence intensity at $\lambda = 550$ nm of **XQS** (3.3×10^{-4} M) upon addition of Zn^{2+} in CH_3CN -PBS (10 mM, v/v=7:3, pH = 7.4). $\lambda_{\text{ex}} = 525$ nm

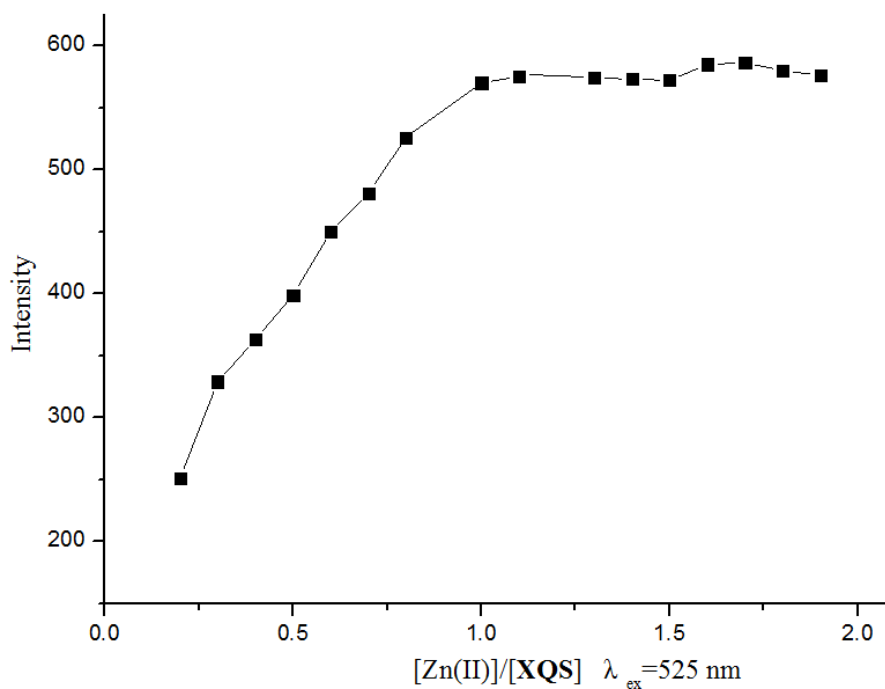


Fig. 5 A plot of fluorescence intensity at 550nm depending on the concentration of Zn^{2+} in the range from 0 to 1.8 equivalents ($\lambda_{\text{ex}} = 525$ nm).

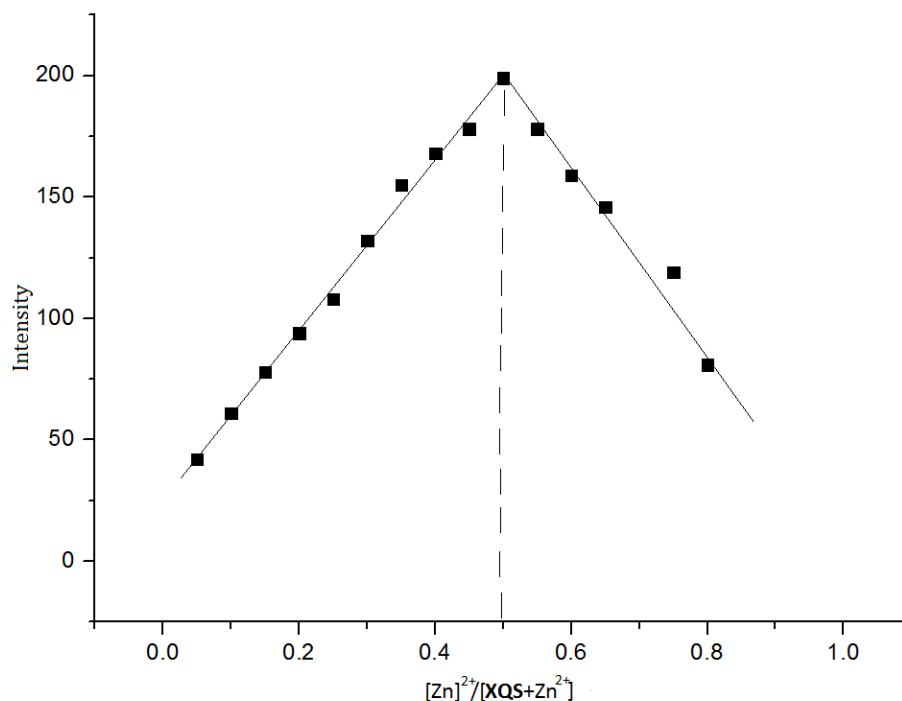


Fig. S6 Job' plot for determination of the binding stoichiometry of probe **XQS** with Zn^{2+} in the presence of Zn^{2+} with different mole ratios of $[Zn^{2+}]/([Zn^{2+}]+[XQS])$ at the constant total concentration ($[Zn^{2+}] + [XQS] = 6.6 \times 10^{-4} M$) at $\lambda = 550$ nm in CH_3CN -PBS (10 mM, v/v=7:3, pH = 7.4), $\lambda_{ex} = 525$ nm.

Table S1 Comparison of detection limits and fluorescence lifetime

The detection limits of **XQS** towards Zn^{2+} in CH_3CN were determined from the following equation:

$$DL = 3 \cdot SD / S$$

Where SD is the standard deviation of the blank solution (**XQS**, 10 μM) detected for 10 times; S is the slope of the calibration curve.

Binding constant was calculated according to the Benesi-Hildebrand equation. K_a was calculated following the equation stated below.

$$1/(F-F_0) = 1/\{K_a(F_{max} - F_0) [Zn^{2+}]\} + 1/[F_{max}-F_0]$$

Here F_0 , F and F_{max} indicate the emission in absence of, at intermediate and at infinite concentration of metal ion respectively. The binding constant K_a is determined from the ratio of intercept and slope of Benesi-Hildebrand plot. Plot of $1/[F-F_0]$ vs $1/[Zn^{2+}]$ gives a straight line indicating 1:1 complexation between **XQS** and Zn^{2+} .

Probe	Standard Deviation	Slope	(3×Standard deviation)/S lope	Detection Limit	Fluorescence Lifetime (Probes+ Zn^{2+})	Fluorescence quantum yield (Probes+ Zn^{2+})	The binding constant
XQS	0.16	69655.28048 M^{-1}	6.89×10^{-6}	6.89 μM	3.44 ns	61.71 %	$2.8 \times 10^4 M^{-1}$

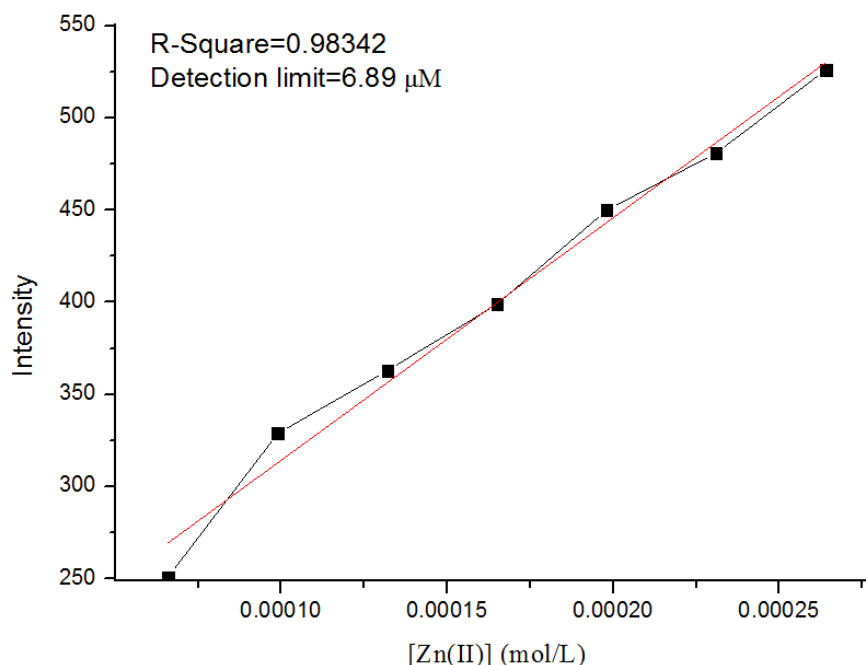


Fig. S7 Detection limit of XQS (3.3×10^{-4} M) towards the detection of Zn^{2+} , $\lambda_{\text{ex}} = 525$ nm

ACKNOWLEDGEMENTS

This work was supported by the National Natural Science Foundation of China (NSFC) (No. 21302019 and 21171040), the Key Projects of Natural Science Research of Anhui Province Colleges and Universities (No. KJ2018A0338 and No. KJ2018A0337), the Key Projects of Support Program for Outstanding Young Talents in Anhui Province Colleges and Universities (No. gxyqZD2016068), National Undergraduate Training Programs for Innovation and Entrepreneurship (No. 201710371020), the Innovation Training Program for the Anhui College Students (No. 201710371089), and the Key Natural Science Research Projects of Fuyang Normal University (No. 2017FSKJ06ZD), and the Horizontal Cooperation Project of Fuyang Municipal Government-Fuyang Normal University (No. XDHX201730 and No. XDHX201731).

References

1. Z. Dong, Y. Guo, X. Tian and J. Ma, *J. Lumin.*, 134 (2013) 635.
2. C.K. Kumar, R. Trivedi, L. Giribabu, S. Niveditha, K. Bhanuprakash and B. Sridhar, *J. Organomet. Chem.*, 780 (2015) 20.
3. M.M. Li, S.Y. Huang, H. Ye, F. Ge, J.Y. Miao and B.X. Zhao, *J. Fluoresc.*, 23 (2013) 799.
4. K. Boonkitpatarakul, J. Wang, N. Niamnont, B. Liu, L. McDonald, Y. Pang and M. Sukwattanasinitt, *ACS Sens.*, 1 (2016) 144.
5. B. Valeur and I. Leray, *Chem. Soc. Rev.*, 205 (2000) 3.
6. S. Cao, Q. Jin, L. Geng, L. Mu and S. Dong, *New J. Chem.*, 40 (2016) 6264.
7. M.J. Chang and M.H. Lee, *Dyes Pigm.*, 149 (2018) 915.
8. S. Guang, G. Wei, Z. Yan, Y. Zhang, G. Zhao, R. Wu and H. Xu, *Analyst*, 143 (2018) 449.
9. R.S. Kumar, S.K.A. Kumar, K. Vijayakrishna, A. Sivaramakrishna, P. Paira, C.V.S. Brahmmananada Rao, N. Sivaramanb and S.K. Sahoo, *New J. Chem.*, 42 (2018) 8494.
10. C. Bazzicalupi, A. Bencini and V. Lippolis, *Chem. Soc. Rev.*, 39 (2010) 3709.
11. A.I. Bush, W.H. Pettingell, G. Multhaupt, M.d. Paradis, J.P. Vonsattel, J.F. Gusella, K. Beyreuther, C.L. Masters and R.E. Tanzi, *Science*, 265 (1994) 1464.
12. V. Bhalla and M. Kumar, *Dalton Trans.*, 42 (2013) 975.

13. M. Sohrabi, M. Amirnasr, H. Farrokhpour and S. Meghdadi, *Sens. Actuators B Chem.*, 250 (2017) 647.
14. K. Tayade, S.K. Sahoo, B. Bondhopadhyay, V.K. Bhardwaj, N. Singh, A. Basu, R. Bendre and A. Kuwar, *Biosens. Bioelectron.*, 61 (2014) 429.
15. M. Zhang, W. Lu, J. Zhou, G. Du, L. Jiang, J. Ling and Z. Shen, *Tetrahedron*, 70 (2014) 1011.
16. W. Cao, X.-J. Zheng, J.-P. Sun, W.-T. Wong, D.-C. Fang, J.-X. Zhang and L.-P. Jin, *Inorg. Chem.*, 53 (2014) 3012.
17. S. Erdemir, M. Yuksekogul, S. Karakurt and O. Kocyigit, *Sens. Actuators B Chem.*, 241 (2017) 230.
18. W.K. Dong, S.F. Akogun, Y. Zhang, Y.X. Sun and X.-Y. Dong, *Sens. Actuators B Chem.*, 238 (2017) 723.
19. H. Kang, C. Fan, H. Xu, G. Liu and S. Pu, *Tetrahedron*, 74 (2018) 4390.
20. S.W. Jia, H. In-Chul, S.K. Kwang and S.K. Jong, *Org. Lett.*, 9 (2007) 907.
21. M. Ozdemir, *Spectrochim. Acta A.*, 161 (2016) 115.
22. X.Q. Hu, J. Chai, Y.F. Liu, B. Liu and B.S. Yang, *Spectrochim. Acta A.*, 153 (2016) 505.
23. J. Li, C. Yin and F. Huo, *Dyes Pigm.*, 131 (2016) 100.
24. K.P. Wang, Z.H. Jin, H.S. Shang, C.D. Lv, Q. Zhang, S. Chen and Z-Q. Hu, *J. Fluoresc.*, 27 (2017) 629.
25. Z. Yang, Y. Zhao, S. Chen, Y. Bu, X. Zhu, Y. Du and F. Li, *Sens. Actuators B Chem.*, 235 (2016) 414.
26. M. Devi, A. Dhir and C.P. Pradeep, *RSC Adv.*, 6 (2016) 112728.
27. V.K. Gupta, *Int. J. Electrochem. Sci.*, 10 (2015) 7854.
28. V.K. Gupta, *Int. J. Electrochem. Sci.*, 11 (2016) 1640.

© 2018 The Authors. Published by ESG (www.electrochemsci.org). This article is an open access article distributed under the terms and conditions of the Creative Commons Attribution license (<http://creativecommons.org/licenses/by/4.0/>).